European Journal of Operational Research 281 (2020) 174–185

Contents lists available at ScienceDirect

European Journal of Operational Research

journal homepage: www.elsevier.com/locate/ejor

Innovative Applications of O.R.

A second-order cone model of transmission planning with alternating and direct current lines☆

Antoine Lesage-Landry*, Joshua A. Taylor

The Edward S. Rogers Sr. Department of Electrical and Computer Engineering, University of Toronto, 10 King's College Road, Toronto, Ontario M5S 3G4 Canada

ARTICLE INFO

Article history:
Received 20 February 2019
Accepted 7 August 2019
Available online 13 August 2019

Keywords:
OR in energy
Electric power systems
Transmission expansion planning
Mixed-integer second-order cone programming
Convex relaxation

ABSTRACT

We construct a model for transmission planning with both alternating and direct current lines, the latter of which can be interfaced via either line-commutated converters or voltage-source converters. The transmission expansion problem is nonlinear and nonconvex. Thus, nonlinear solvers cannot guarantee their convergence to the global optimum of the problem. We use relaxations and approximations to formulate a mixed-integer second-order cone transmission expansion model, which can be solved to optimality by current industrial solvers. We base our formulation on the branch flow relaxation. We include losses and reactive power placement, and consider direct current lines connected by both line-commutated converters and voltage-sourced converters. We show that our approach lowers the expansion cost on 6-bus and 24-bus system examples. We evaluate the feasibility of our formulation using a semidefinite relaxation of optimal power flow and find that the resulting plan admits feasible or close to feasible power flows.

1. Introduction

Electric power grids periodically need new transmission lines to accommodate new demand and generation (Hemmati, Hooshmand, & Khodabakhshian, 2013; Lumbreras & Ramos, 2016). Most of the existing literature on transmission expansion planning focuses strictly on alternating current (AC) lines. Direct current (DC) transmission lines have many advantages over AC lines, including lower costs and losses over long distances, better wire utilization, and greater controllability (Bahrman & Johnson, 2007; Barnes, Van Hertem, Teeuwsen, & Callavik, 2017; Dominguez, Macedo, Escobar, & Romero, 2017; Ghadiri, Haghifam, & Larimi, 2017). Additional advantages, which are not typically accounted for in steady state planning models, include the ability to interface asynchronous networks and improved controllability (Bahrman & Johnson, 2007; Barnes et al., 2017; Henderson et al., 2007).

In this work, we formulate an AC–DC transmission planning model in which the decision maker must satisfy generation, demand, and network constraints by building both AC and DC lines. We also allow conversion of existing lines from AC to DC. Voltage-sourced converters (VSCs) or line-commutated converters (LCCs) must be added to interface new DC lines. Transmission expansion planning is nonconvex due to power flow, discrete line and converter installation variables, and products between the power flow variables and installation variables (Taylor & Hover, 2013). As a result, approximations are necessary to make transmission planning tractable. In this work, we formulate a mixed-integer second-order cone (MISOC) AC–DC transmission expansion planning model. The model can be solved to optimality using commercial software. We note that relaxation-based models can lead to plans that are infeasible with respect to the original nonconvex expansion problem. In numerical examples, we found that any expansion plans that did not admit a feasible power flow solution could be easily made feasible with the addition of a small number of lines and converters.

Related work. Several recent papers have investigated power flow in networks with AC and DC lines. Refs. Beerten, Cole, and Belmans (2012), Cao, Du, Wang, and Bu (2013), Feng, Le Tuan, Tjernberg, Mannikoff, and Bergman (2014), Schilling, Kuschke, and Strunz (2017), and Ahmed, Eltantawy, and Salama (2018a) solve nonconvex models with nonlinear programming. Refs. Urquidez and Xie (2015) and Yang, Zhong, Bose, Xia, and Kang (2018) formulated linear approximations of AC–DC optimal power flow. Second-order cone and semidefinite convex relaxations of the AC–DC optimal power flow were investigated in Baradar, Hesamzadeh, and Ghandhari (2013), Ergun, Dave, Van Hertem, and Geth (2019) and Bahrami, Therrien, Wong, and Jatskevich (2017), respectively.

☆ This work was funded by the Fonds de recherche du Québec – Nature et technologies, the Ontario Ministry of Research, Innovation and Science and the Natural Sciences and Engineering Research Council of Canada.

* Corresponding author.
E-mail addresses: alandry@ece.utoronto.ca (A. Lesage-Landry), josh.taylor@utoronto.ca (J.A. Taylor).

https://doi.org/10.1016/j.ejor.2019.08.016
0377-2217/

Transmission expansion planning using only AC transmission lines is an established topic in the literature. The main challenges are: (i) the nonconvexity of power flow, (ii) discrete expansion variables, and (iii) nonconvex products between expansion and power flow variables. Convex relaxations were used to overcome these challenges in the AC case in Ghaddar and Jabr (2019); Taylor and Hover (2013).

AC–DC transmission expansion planning has also been a topic of recent interest. Heuristic-based approaches were proposed in Doagou-Mojarrad, Rastegar, and Gharehpetian (2016), Ghadiri et al. (2017), Wu, Liu, Gu, Huang, and Han (2018), and Ahmed, Eltantawy, and Salama (2018b), most of which combines a mathematical programming step with a heuristic algorithm. Mixed-integer linear programming (MILP)-based approaches for AC–DC transmission expansion planning have also been proposed. MILPs are nonconvex but can be solved efficiently when there are a moderate number of integer variables. Linearized power flow and Benders' decomposition were used in Lotfjou, Fu, and Shahidehpour (2012). To improve on the accuracy of the power flow model, piece-wise linearization was used in Dominguez et al. (2017); Dominguez, Zuluaga, Macedo, and Romero (2016). In Frank and Rebennack (2015), a mixed-integer quadratically constrained program is given for optimizing the electrical layout of a building with AC and DC lines, and is solved using a nonconvex Benders' decomposition. In (Novoa & Rios, 2017), conversion of lines from AC to DC is optimized using a heuristic approach.

To the best of our knowledge, only Frank and Rebennack (2015) and Wu et al. (2018) used convex relaxations in the context of AC–DC expansion planning. In Frank and Rebennack (2015), McCormick inequalities (McCormick, 1976), which require iterative constraint tightening, were used to relax bilinear and quadratic equality constraints and obtain lower bounds for the nonconvex generalized Benders decomposition. In Wu et al. (2018), a second-order cone relaxation (SOCR) of power flow is used, but the resulting problem is still nonconvex due to product between power flow and installation variables, and the resulting problem is solved using a genetic algorithm. In this work, we formulate the first mixed-integer second-order cone model for mixed AC–DC transmission expansion planning, which can be solved as written to optimality by industrial solvers like `Gurobi` (Gurobi Optimization, 2018).

Our specific contributions are as follows.

- We construct a new MISOC model for AC–DC transmission expansion planning. By fixing the voltage magnitudes in the second-order cone (SOC) branch flow relaxation to one, we obtain an MISOC AC–DC transmission expansion planning model. A similar approach was previously used in Taylor and Hover (2013) for purely AC transmission expansion planning. Ours is the first model that allows for the addition of AC and DC lines with both VSC and LCC converters, reactive power support, and conversion of AC lines to DC. We also model reactive power, line and converter losses, and make no general assumptions to restrict the network topology. The new model has approximately twice the number of variables and constraints as conventional optimal power flow, whereas an approach based purely on relaxations could have orders of magnitude more.
- We apply the new model in 6-bus and 24-bus case-studies. We use the semidefinite relaxation of AC–DC power flow in Bahrami et al. (2017) to evaluate the feasibility of the resulting plan. When the optimal plan is infeasible, we show that minor reinforcement can be used to attain feasibility with respect to the exact constraints.
- We find in our case studies that the inclusion of DC lines in transmission expansion can produce solutions that cost as little as half as much as those obtained when only AC lines are permitted.

Table 1
Network parameter definition (for all $i \in \mathcal{N}$, $ij \in \mathcal{L}$ and $t = 1, 2, \ldots, T$).

Parameter	Description
$\overline{p}_i \in \mathbb{R}$	Maximum active power at node i [MW]
$\underline{p}_i \in \mathbb{R}$	Minimum active power at node i [MW]
$\overline{q}_i \in \mathbb{R}$	Maximum reactive power at node i [MVAR]
$\underline{q}_i \in \mathbb{R}$	Minimum reactive power at node i [MVAR]
$\overline{v}_{ij}^{\mathrm{AC}} \in \mathbb{N}$	Maximum number of new AC lines
$\overline{v}_{ij}^{\mathrm{DC}} \in \mathbb{N}$	Maximum number of new DC lines
$\overline{v}_i \in \mathbb{R}$	Maximum voltage magnitude at bus i [V]
$\underline{v}_i \in \mathbb{R}$	Minimum voltage magnitude at bus i [V]
$\overline{S}_{ij}^{\mathrm{AC}} \in \mathbb{R}_+$	Maximum apparent AC power of line ij [MVA]
$\overline{S}_{ij}^{\mathrm{DC}} \in \mathbb{R}_+$	Maximum apparent DC power of line ij [MVA]
$R_{ij} \in \mathbb{R}_+$	Resistance of line ij [Ω]
$X_{ij} \in \mathbb{R}_+$	Susceptance of line ij [Ω^{-1}]
$Y_{ij} \in \mathbb{R}_+$	Admittance of line ij [Ω^{-1}]
$R_{ij}^{\mathrm{DC}} \in \mathbb{R}_+$	Resistance of DC line ij [Ω]
$Y_{ij}^{\mathrm{DC}} \in \mathbb{R}_+$	Admittance of DC line ij [Ω^{-1}]
$\overline{I}_i \in \mathbb{R}_+$	Maximum current magnitude the VSCs at node i [A]
$\overline{J}_i \in \mathbb{R}_+$	Maximum current magnitude the LCCs at node i [A]
$a_i^{\mathrm{VSC},\cdot}$, $b_i^{\mathrm{VSC},\cdot}$, $c_i^{\mathrm{VSC},\cdot} \geq 0$	VSC loss coefficients at node i [MW,MW/A,MW/A^2]
$a_i^{\mathrm{LCC},\cdot}$, $b_i^{\mathrm{LCC},\cdot}$, $c_i^{\mathrm{LCC},\cdot} \geq 0$	LCC loss coefficients at node i for inverters or rectifiers [MW,MW/A,MW/A^2]
$\nu_{ij}^{0,\mathrm{AC}} \in \mathbb{N}$	Amount of already existing AC line ij
$\nu_{ij}^{0,\mathrm{DC}} \in \mathbb{N}$	Amount of already existing DC line ij
$\overline{v}_{ij}^{\mathrm{AC}} \in \mathbb{N}$	Maximum of AC lines in corridor ij
$\overline{v}_{ij}^{\mathrm{DC}} \in \mathbb{N}$	Maximum of DC lines in corridor ij
$n_i^{0,\mathrm{VSC}} \in \mathbb{N}$	Amount of already existing VSCs at node i
$n_i^{0,\mathrm{LCC}} \in \mathbb{N}$	Amount of already existing LCCs at node i
$\overline{n}_i^{\mathrm{VSC}} \in \mathbb{N}$	Maximum of VSC at node i
$\overline{n}_i^{\mathrm{LCC}} \in \mathbb{N}$	Maximum of LCC at node i
$x_i^0 \in \mathbb{R}_+$	Initial reactance of capacitor bank at node i [Ω]
$s_i^0 \in \mathbb{R}_+$	Initial susceptance of phase reactor at node i [Ω^{-1}]
$\overline{x} \in \mathbb{R}_+$	Maximum reactance of a capacitor bank [Ω]
$\overline{s} \in \mathbb{R}_+$	Maximum susceptance of a phase reactor [Ω^{-1}]
a_i^g, b_i^g, $c_i^g \geq 0$	Power generator cost coefficients at node i [M$, M$/MW,M$/MW^2]
$\overline{g}_{p,i} \in \mathbb{R}_+$	Maximum active power generation at node i [MW]
$\overline{g}_{q,i} \in \mathbb{R}$	Maximum reactive power generation at node i [MVAR]
$\underline{g}_{q,i} \in \mathbb{R}_+$	Minimum reactive power generation at node i [MW]
$\overline{g}_{p,i}^{\mathrm{DC}} \in \mathbb{R}_+$	Maximum DC power generation at node i [MW]
$d_{p,i}^t \in \mathbb{R}_+$	Active power demand at node i [MW]
$d_{q,i}^t \in \mathbb{R}$	Reactive power demand at node i [MVAR]
$d_i^{t,\mathrm{DC}} \in \mathbb{R}$	DC power demand at node i [MW]
$c_i^{\mathrm{cb},0}$, c_i^{cb}, $c_i^{\mathrm{b}} \geq 0$	Capacitor bank/phase reactor cost coefficient [M$, M$/MVAR, M$/MVAR]

2. Transmission system planning

2.1. Notation

Let $\mathcal{N}$ and $\mathcal{L}$ denote the sets of nodes and lines in the network. A single subscript, $i \in \mathcal{N}$, appended to a parameter or variable refers to a node. A double subscript, $ij \in \mathcal{L}$, refers to the line corridor between node i and j. If a line exists or can be built, then $ij \in \mathcal{L}$. Let $\mathcal{E}$ be the set of existing lines before the expansion.

We allow for multiple scenarios to accommodate for varying load and generation and to reflect the constraints of LCCs. We let a superscript $t = 1, 2, \ldots, T$ refer to the scenario. The full notation is summarized in Tables 1, 2 and 3.

2.2. Expansion rules

In this section, we state the logical rules that constrain the expansion of an AC–DC transmission system. We model every node

Table 2
Continuous variable definition for scenario t (for all $i \in \mathcal{N}$, $ij \in \mathcal{L}$ and $t = 1, 2, \ldots, T$).

Variable	Description
$v_i \in \mathbb{C}$	Voltage at node i [V]
$I_{ij} \in \mathbb{C}$	Current in line ij [A]
$I_i \in \mathbb{C}$	Current in converter at node i [A]
$P_{ij}^t \in \mathbb{R}$	Active power in AC line ij [MW]
$Q_{ij}^t \in \mathbb{R}$	Reactive power in AC line ij [MVAR]
$P_{ij}^{t,\mathrm{DC}} \in \mathbb{R}$	Active power in DC line ij [MW]
$p_i^t \in \mathbb{R}$	Active power at node i [MW]
$q_i^t \in \mathbb{R}$	Reactive power at node i [MVAR]
$p_i^{t,\mathrm{DC}} \in \mathbb{R}$	Active power at DC node i [MW]
$p_i^{t,\mathrm{toDC}} \in \mathbb{R}$	AC active power converted to DC at node i [MW]
$q_i^{t,\mathrm{toDC}} \in \mathbb{R}$	Reactive power absorbed by the converter at node i [MVAR]
$p_i^{t,\mathrm{toAC}} \in \mathbb{R}$	DC power converted to AC active power at node i [MW]
$p_i^{t,\mathrm{VSC,loss,AC-DC}} \in \mathbb{R}$	AC–DC VSC power converter losses at node i [MW]
$p_i^{t,\mathrm{LCC,loss,AC-DC}} \in \mathbb{R}$	AC–DC LCC power converter losses at node i [MW]
$p_i^{t,\mathrm{VSC,loss,DC-AC}} \in \mathbb{R}$	DC–AC VSC power converter losses at node i [MW]
$p_i^{t,\mathrm{LCC,loss,DC-AC}} \in \mathbb{R}$	DC–AC LCC power converter losses at node i [MW]
$\phi_{ij}^{\mathrm{AC-DC}} \in \mathbb{R}$	AC to DC ij line conversion indicator ($1 \triangleq$ line is converted to DC & $0 \triangleq$ no conversion)
$\tau_{ij} \in \mathbb{R}^N$	Intermediary variable for point-to-point bilinear constraint
$x_i \in \mathbb{R}$	Capacitor bank reactance added at node i [Ω]
$s_i \in \mathbb{R}$	Phase reactor susceptance added at node i [Ω^{-1}]
$g_{p,i}^t \in \mathbb{R}_+$	Active power generation at node i [MW]
$g_{q,i}^t \in \mathbb{R}$	Reactive power generation at node i [MVAR]
$g_i^{t,\mathrm{DC}} \in \mathbb{R}_+$	DC power generation at node i [MW]
$\ell^t \in \mathbb{R}_+$	Total active power loss at time t [MW]
$\mathbf{V}^t \in \mathbb{C}^{\mathrm{card}\,\mathcal{N} \times \mathrm{card}\,\mathcal{N}}$	Semidefinite voltage variable [V^2]

Table 3
Integer variable definition (for all $i \in \mathcal{N}$, $ij \in \mathcal{L}$ and $t = 1, 2, \ldots, T$).

Variable	Description	Detail
$\mu_{ij}^{\mathrm{AC}} \in \{0, 1\}$	Decision to AC build line ij	$1 \triangleq$ build & $0 \triangleq$ do not build
$\mu_{ij}^{\mathrm{DC}} \in \{0, 1\}$	Decision to DC build line ij	$1 \triangleq$ build & $0 \triangleq$ do not build
$\nu_{ij}^{\mathrm{AC}} \in \mathbb{N}$	Number of AC lines built	
$\nu_{ij}^{\mathrm{DC}} \in \mathbb{N}$	Number of DC lines built	
$\lambda_i \in \{0, 1\}$	Node is AC-enabled	$1 \triangleq$ yes & $0 \triangleq$ no
$\kappa_i \in \{0, 1\}$	Node is DC-enabled	$1 \triangleq$ yes & $0 \triangleq$ no
$\xi_i \in \{0, 1\}$	Presence of a converter at node i	$1 \triangleq$ build converter & $0 \triangleq$ do not build converter
$\eta_i \in \{0, 1\}$	Presence of an LCC converter at node i	$1 \triangleq$ build LCC & $0 \triangleq$ no LCC converter (if $\xi_i = 1$ and $\eta_i = 0$ build VSC)
$\psi_i^t \in \{0, 1\}$	Power flow direction in a converter at node i	$1 \triangleq$ AC to DC & $0 \triangleq$ DC to AC
$n_i^{\mathrm{VSC}} \in \mathbb{N}$	Number of VSCs built at node i	
$n_i^{\mathrm{LCC}} \in \mathbb{N}$	Number of LCCs built at node i	
$\chi_i \in \{0, 1\}$	presence of a capacitor bank at node i	$1 \triangleq$ yes & $0 \triangleq$ no

as having an AC and a DC channel. If a node has both channels active, then a converter must be present.

Let parameter $B_{ij}^0 = 0$ if the existing line in $ij \in \mathcal{E}$ is AC and 1 if it is DC. Let the expansion variable $\mu_{ij}^{\mathrm{AC}} \in \{0, 1\}$ and $\mu_{ij}^{\mathrm{DC}} \in \{0, 1\}$ represent the decisions to build AC and DC lines in corridor ij. These variables can represent building a new line or adding capacity to existing lines. If $\mu_{ij}^{\mathrm{DC}} = 1$ and $B_{ij}^0 = 0$, then the existing AC line at ij is converted to DC, and there is a conversion cost. Although our model can similarly accommodate conversion from DC to AC, we do not include this because it does not occur in practice.

Let $\nu_{ij}^{\mathrm{AC}} \in \mathbb{N}$ and $\nu_{ij}^{\mathrm{DC}} \in \mathbb{N}$ be the quantity of AC and DC lines built. These variables are constrained as follows.

$$\mu_{ij}^{\mathrm{AC}} + \mu_{ij}^{\mathrm{DC}} \leq 1 \tag{1}$$

$$\mu_{ij}^{\mathrm{AC}} \leq \nu_{ij}^{\mathrm{AC}} \leq \mu_{ij}^{\mathrm{AC}} \overline{\nu}_{ij}^{\mathrm{AC}} \tag{2}$$

$$\mu_{ij}^{\mathrm{DC}} \leq \nu_{ij}^{\mathrm{DC}} \leq \mu_{ij}^{\mathrm{DC}} \overline{\nu}_{ij}^{\mathrm{DC}}. \tag{3}$$

Let $\lambda_i \in \{0, 1\}$ be 1 if the AC channel is active and 0 if not. Let $\kappa_i \in \{0, 1\}$ be 1 if the DC channel is active and 0 if not. We then have the following constraints. A node must necessarily be AC, DC or both:

$$\kappa_i + \lambda_i \geq 1. \tag{4}$$

If a node has both channels active, then a converter must be built. Let $\xi_i = 1$ represent the decision to build a converter at node i. Then

$$\xi_i = \kappa_i + \lambda_i - 1. \tag{5}$$

Note that this implies that if a converter is built, $\xi_i = 1$. AC lines can only connect to AC-enabled buses:

$$\mu_{ij}^{\mathrm{AC}} \leq \lambda_i \tag{6}$$

$$\mu_{ij}^{\mathrm{AC}} \leq \lambda_j. \tag{7}$$

DC lines can only connect to DC-enabled buses:

$$\mu_{ij}^{\mathrm{DC}} \leq \kappa_i \tag{8}$$

$$\mu_{ij}^{\mathrm{DC}} \leq \kappa_j. \tag{9}$$

Let the continuous variable $\phi_{ij}^{\mathrm{AC-DC}}$ indicate that an existing line is converted from AC to DC. This variables is later used to compute the cost of the expansion. It does not depend on the size of the candidate line. For $ij \in \mathcal{E}$, we have

$$\mu_{ij}^{\mathrm{DC}} - B_{ij}^0 \leq \phi_{ij}^{\mathrm{AC-DC}} \tag{10}$$

$$0 \leq \phi_{ij}^{\mathrm{AC-DC}} \leq \mu_{ij}^{\mathrm{DC}}. \tag{11}$$

While $\phi_{ij}^{\mathrm{AC-DC}}$ is continuous, it will only take the value of zero, if no conversion occurs, or one if a conversion occurs. If no line exist in a corridor ij, then $\phi_{ij}^{\mathrm{AC-DC}} = 0$. Similarly, if $B_{ij}^0 = 1$, the existing line in corridor ij is already DC, and conversion is not an option.

2.3. AC expansion

We use the branch flow relaxation (Taylor, 2015) to model the AC portion of the network. We use the SOC approximation presented in Taylor and Hover (2013) to model the AC transmission expansion planning problem. The main assumptions are (i) the voltage magnitude of all AC nodes is equal to 1 per unit, and (ii) some power equality constraints directly related to costs are relaxed to inequality. The second assumption is mild because increasing losses usually increases the objective function and thus the constraint will be active. The resulting model is essentially network flow with line losses that depend quadratically on the flows.

Let P_{ij} and Q_{ij} be, respectively, the active and reactive power flowing from node i to j. Denote p_i and q_i as the active and reactive power going into or out of node i. We use the convention that $p_i > 0$ indicates that power flows into the node. Let R_{ij} and X_{ij} be the resistance and reactance of the line ij.

The constraints of the AC portion of our model are:

$$R_{ij}(P_{ij}^{t2} + Q_{ij}^{t2}) \leq (P_{ij}^{t} + P_{ji}^{t})(\nu_{ij}^{0,\mathrm{AC}} + \nu_{ij}^{\mathrm{AC}}) \tag{12}$$

$$X_{ij}(P_{ij}^{t2} + Q_{ij}^{t2}) \leq (Q_{ij}^{t} + Q_{ji}^{t})(\nu_{ij}^{0,\mathrm{AC}} + \nu_{ij}^{\mathrm{AC}}) \tag{13}$$

$$p_i^t = \sum_{j:ij\in\mathcal{L}} P_{ij}^t \tag{14}$$

$$q_i^t = \sum_{j:ij\in\mathcal{L}} Q_{ij}^t \tag{15}$$

$$\underline{p}_i \leq p_i^t \leq \overline{p}_i \tag{16}$$

$$\underline{q}_i \leq q_i^t \leq \overline{q}_i \tag{17}$$

$$P_{ji}^{t2} + Q_{ji}^{t2} \leq \overline{S}_{ij}^2(\nu_{ij}^{0,\mathrm{AC}} + \nu_{ij}^{\mathrm{AC}})^2 \tag{18}$$

where $\nu_{ij}^{0,\mathrm{AC}}$ is initial number of lines in corridor ij. Constraints (12) and (13) are SOC constraints, (18) is a convex quadratic constraint, and the rest are linear constraints. We append to (12)–(18) the following constraints to ensure that AC power only flows in AC lines. Recall that B_{ij}^0 indicates the type of already existing lines. For lines $ij \in \mathcal{E}$, we have

$$\left|P_{ij}^t\right| \leq L_{ij}\left(1 - B_{ij}^0 - \phi_{ij}^{\mathrm{AC-DC}}\right) \tag{19}$$

$$\left|Q_{ij}^t\right| \leq L_{ij}\left(1 - B_{ij}^0 - \phi_{ij}^{\mathrm{AC-DC}}\right), \tag{20}$$

where L_{ij} is a large positive scalar. For all the other lines $ij \in \mathcal{L}\setminus\mathcal{E}$, we have

$$\left|P_{ij}^t\right| \leq L_{ij}\mu_{ij}^{\mathrm{AC}} \tag{21}$$

$$\left|Q_{ij}^t\right| \leq L_{ij}\mu_{ij}^{\mathrm{AC}}. \tag{22}$$

2.4. DC expansion

We use a similar approach for the DC part of the network. We add a DC superscript to all variables or parameters used in Section 2.3 to denote the DC quantities.

2.4.1. DC branch flow model

We first derive a DC branch flow model. We follow the approach of Taylor (2015, Chapter 3). The power flowing from node i to j is:

$$\begin{aligned} P_{ij}^{\mathrm{DC}} &= I_{ij}\nu_i \\ &= I_{ij}^2 R_{ij}. \end{aligned}$$

Substituting, we have

$$I_{ij}^2 R_{ij} = \left(\frac{P_{ij}^{\mathrm{DC}}}{\nu_i}\right)^2 R_{ij},$$

and,

$$I_{ij}^2\nu_i^2 = \left(P_{ij}^{\mathrm{DC}}\right)^2.$$

Similarly to the AC case, we let $\gamma_{ij} = I_{ij}^2$ and $\omega_i = \nu_i^2$. Note that because I_{ij} and ν_i are real, no angle information is lost in working instead with γ_{ij} and ω_i. We then obtain

$$\gamma_{ij}\omega_i = \left(P_{ij}^{\mathrm{DC}}\right)^2.$$

Next, the losses of a line are given by the sum of the power at either ends of a line, that is

$$P_{ij}^{\mathrm{DC}} + P_{ji}^{\mathrm{DC}} = R_{ij}I_{ij}^2,$$

or, using the new variables

$$P_{ij}^{\mathrm{DC}} + P_{ji}^{\mathrm{DC}} = R_{ij}\gamma_{ij}.$$

The third equation follows from Ohm's law:

$$\nu_j = \nu_i - R_{ij}I_{ij}.$$

Taking the square of both sides we have:

$$\nu_j^2 = \nu_i^2 - 2\nu_i R_{ij}I_{ij} + R_{ij}^2 I_{ij}^2.$$

Substituting ω_i, γ_{ij} and $P_{ij}^{\mathrm{DC}} = I_{ij}\nu_i$ into the previous equation leads to

$$\omega_j = \omega_i - 2R_{ij}P_{ij}^{\mathrm{DC}} + R_{ij}^2\gamma_{ij}.$$

The DC branch flow model is therefore given by:

$$\gamma_{ij}\omega_i = \left(P_{ij}^{\mathrm{DC}}\right)^2 \tag{23}$$

$$P_{ij}^{\mathrm{DC}} + P_{ji}^{\mathrm{DC}} = R_{ij}\gamma_{ij} \tag{24}$$

$$\omega_j = \omega_i - 2R_{ij}P_{ij}^{\mathrm{DC}} + R_{ij}^2\gamma_{ij}. \tag{25}$$

2.4.2. Expansion

We now incorporate transmission expansion into the DC branch flow model. We use the fact that $\gamma_{ij} = (P_{ij}^{\mathrm{DC}})^2/\omega_i$ and the assumption that $\nu_i = \omega_i = 1$ per unit for all i. Note that because all voltages are the same, (25) is omitted. The line losses constraint (24) for scenario t becomes:

$$P_{ij}^{t,\mathrm{DC}} + P_{ji}^{t,\mathrm{DC}} = R_{ij}\left(P_{ij}^{t,\mathrm{DC}}\right)^2,$$

which is not convex. We relax this equality to an inequality constraint:

$$P_{ij}^{t,\mathrm{DC}} + P_{ji}^{t,\mathrm{DC}} \geq R_{ij}\left(P_{ij}^{t,\mathrm{DC}}\right)^2. \tag{26}$$

We remark that this relaxation rarely changes the optimum because increasing losses usually increases the objective (Taylor & Hover, 2013). Using (26), the constraints for the DC transmission system planning are:

$$R_{ij}\left(P_{ij}^{t,\mathrm{DC}}\right)^2 \leq (P_{ij}^{t,\mathrm{DC}} + P_{ji}^{t,\mathrm{DC}})(\nu_{ij}^{0,\mathrm{DC}} + \nu_{ij}^{\mathrm{DC}}) \tag{27}$$

$$p_i^{t,\mathrm{DC}} = \sum_{j:ij\in\mathcal{L}} P_{ij}^{t,\mathrm{DC}} \tag{28}$$

$$\underline{p}_i^{\mathrm{DC}} \leq p_i^{t,\mathrm{DC}} \leq \overline{p}_i^{\mathrm{DC}} \tag{29}$$

$$\left|P_{ij}^{t,\mathrm{DC}}\right| \leq \overline{S}_{ij}^{\mathrm{DC}}\left(\nu_{ij}^{0,\mathrm{DC}} + \nu_{ij}^{\mathrm{DC}}\right) \tag{30}$$

where the parameter $\nu_{ij}^{0,\mathrm{DC}}$ represents initial number of lines in corridor ij. Like (12) and (13), (27) is SOC, and the rest of the constraints are linear. Similarly to the AC case, we also have the following constraints to ensure that DC power only flows in DC lines. For already existing lines, $ij \in \mathcal{E}$, we have

$$\left|P_{ij}^{t,\mathrm{DC}}\right| \leq L_{ij}\left(B_{ij}^0 - \phi_{ij}^{\mathrm{AC-DC}}\right). \tag{31}$$

For all the other lines, $ij \in \mathcal{L}\setminus\mathcal{E}$, we have

$$\left|P_{ij}^{t,\mathrm{DC}}\right| \leq L_{ij}\mu_{ij}^{\mathrm{DC}}. \tag{32}$$

2.5. Converters

Throughout this section we let $i \in \mathcal{N}$ denote a node with a converter. Power-electronic converters are necessary to interface AC and DC lines. We consider VSCs and LCCs. Let $p_i^{t,\mathrm{toDC}} \in \mathbb{R}$ and $p_i^{t,\mathrm{toAC}} \in \mathbb{R}$ be the power flowing thought a converter at node i. These variables represent the AC power converted to DC and the DC power converted to AC, respectively. Let $q_i^{t,\mathrm{toDC}} \in \mathbb{R}$ be the reactive power absorbed by an AC–DC converter.

2.5.1. VSC

A VSC can be used in two configurations: as a rectifier for AC to DC conversion or as an inverter for DC to AC power conversion. Let $\psi_i^t = 1$ if the converter is a AC–DC converter at time t and 0 if it is a DC–AC converter. If there is no converter at node i, ψ_i^t has no effect on the problem. If a VSC is used, its configuration at time t is given by:

$$p_i^{t,\text{toDC}} \leq M\psi_i^t \tag{33}$$

$$p_i^{t,\text{toDC}} \geq M(\psi_i^t - 1). \tag{34}$$

The active and reactive power flowing through the converter are limited by its apparent power capacity via the maximum current $\bar{I}$ the converter can handle (Bahrami et al., 2017). It thus follows that for all t:

$$\begin{aligned}\left(p_i^{t,\text{toDC}}\right)^2 + \left(q_i^{t,\text{toDC}}\right)^2 &= S_i^2,\\ &\leq \bar{I}_i^2,\end{aligned} \tag{35}$$

because we have assumed one per unit voltage magnitudes. The reactive power absorbed by the converter is bounded above at all t by Bahrami et al. (2017), Feng et al. (2014):

$$q_i^{t,\text{toDC}} \leq \alpha_i S_i^{\text{c,nominal}},$$

where $S_i^{\text{c,nominal}}$ is the nominal apparent power of the converter at i and α is a positive scalar that depends on the converter. Assuming that the difference in phase angles between the converter and filter voltages is small (Bahrami et al., 2017), the reactive power that can be injected by the converter is bounded below by:

$$q_i^{t,\text{toDC}} \geq -|B_i|\overline{v}_i\left(\overline{v}_i - \left|v_f\right|\right),$$

where B_i is the susceptance of the non-ideal phase reactor at the converter node i. Because we've assumed that all nodal voltages are one per unit, this becomes

$$q_i^{t,\text{toDC}} \geq -|B_i|\overline{v}_i(\overline{v}_i - 1). \tag{36}$$

The phase reactor can be sized to satisfy expansion requirements. Let $s_i \in \mathbb{R}$, a continuous variable, be the susceptance magnitude of the non-ideal phase reactor at converter node i and s_i^0 be its base value. We re-express (36) as

$$\begin{aligned} q_i^{t,\text{toDC}} &\geq -(s_i^0 + s_i)\overline{v}_i(\overline{v}_i - 1)\\ s_i &\leq \bar{s}\\ s_i &\geq 0,\end{aligned}$$

where $\bar{s}$ is the maximum size of the phase reactor susceptance.

The real power balance for the converter at a node at i and scenario t is:

$$p_i^{t,\text{toDC}} - p_i^{t,\text{VSC,loss,AC–DC}} = -p_i^{t,\text{toAC}} + p_i^{t,\text{VSC,loss,DC–AC}}.$$

Below, we give convex approximations for $p_i^{t,\text{VSC,loss,AC–DC}}$ and $p_i^{t,\text{VSC,loss,DC–AC}}$ for all t and i. In Section 2.5.3, we use disjunctive constraints to ensure that only one of them is nonzero.

We compute the losses $p_i^{t,\text{VSC,loss,AC–DC}}$ for an AC–DC converter and $p_i^{t,\text{VSC,loss,DC–AC}}$ for a DC–AC converter at i using a quadratic model (Bahrami et al., 2017; Beerten, Cole, & Belmans, 2010; Daelemans, 2008; Daelemans, Srivastava, Reza, Cole, & Belmans, 2009):

$$\begin{aligned}p_i^{t,\text{converter,loss,direction}} &= a_i^{\text{converter,direction}} + b_i^{\text{converter,direction}}\left|I_i^t\right|\\ &\quad + c_i^{\text{converter,direction}}\left|I_i^t\right|^2,\end{aligned}$$

where $a_i^{\text{converter,direction}}$, $b_i^{\text{converter,direction}}$ and $c_i^{\text{converter,direction}}$ are converter-specific, node-specific, positive parameter (Bahrami et al., 2017; Feng et al., 2014) and I_i the current through the converter. The losses of a power converter must be convexified. We consider the AC–DC case and then extend the result to the DC–AC case. First, we relax the equality to an '$\geq$'. Because an increase in the loss will usually lead to an increase in the objective function, this constraint should be active and therefore equivalent to an equality constraint. Second, we bound above the linear term by

$$\left|I_i^t\right| = \frac{\sqrt{\left(p_i^{t,\text{toDC}}\right)^2 + \left(q_i^{t,\text{toDC}}\right)^2}}{\left|v_i^t\right|} \leq \left|p_i^{t,\text{toDC}}\right| + \left|q_i^{t,\text{toDC}}\right|.$$

where we use the approximation $\left|v_i^t\right| = 1$ for all i and t. We therefore have the following convex quadratic constraint (CQC) for all t:

$$\begin{aligned}p_i^{t,\text{VSC,loss,AC–DC}} &\geq a_i^{\text{VSC,AC–DC}} + b_i^{\text{VSC,AC–DC}}\left(\left|p_i^{t,\text{toDC}}\right| + \left|q_i^{t,\text{toDC}}\right|\right)\\ &\quad + c_i^{\text{VSC,AC–DC}}\left(\left(p_i^{t,\text{toDC}}\right)^2 + \left(q_i^{t,\text{toDC}}\right)^2\right),\end{aligned}$$

for AC–DC VSC and

$$\begin{aligned}p_i^{t,\text{VSC,loss,DC–AC}} &\geq a_i^{\text{VSC,DC–AC}} + b_i^{\text{VSC,DC–AC}}\left(\left|p_i^{t,\text{toAC}}\right| + \left|q_i^{t,\text{toAC}}\right|\right)\\ &\quad + c_i^{\text{VSC,DC–AC}}\left(\left(p_i^{t,\text{toAC}}\right)^2 + \left(q_i^{t,\text{toAC}}\right)^2\right),\end{aligned}$$

for DC–AC VSC where $p_i^{t,\text{toDC}}$ is non-negative.

2.5.2. LCC

LCCs are less expensive than VSCs, but have less flexible operation and a larger footprint, which can make them unsuitable for space-limited applications like offshore wind and urban power infeeds. Let $\eta_i = 1$ denote the decision to build at least one LCC at node i. Recall that $\xi_i = 1$, represents the decision to build a converter at node i. If $\eta_i = 0$ and $\xi_i = 1$, then the converter at node i is a VSC. An LCC can in principle be used as a rectifier or as an inverter. Changing the polarity of an LCCs voltage generally requires de-energizing the converter station (CIGRE B4-52 Working Group, 2011). As a result, it is impractical to change the direction of power flow through an LCC over short time periods. We therefore constrain the power flow through an LCC to be in the same direction in all time periods. This is enforced by:

$$\psi_i^1 \leq \psi_i^t + (1 - \eta_i) \tag{37}$$

$$\psi_i^1 \geq \psi_i^t - (1 - \eta_i), \tag{38}$$

for all $t = 2, 3, \ldots, T$ and $i \in \mathcal{N}$. When used as inverters, LCCs can experience commutation failures, which can compromise grid stability (CIGRE B4-52 Working Group, 2011). The following constraint can be added to the expansion problem to prohibit LCCs from acting as inverters:

$$\psi_i^t \geq \eta_i. \tag{39}$$

For increased reliability, we can also restrict LCCs at generation nodes. Constraint (39) is optional because modern LCC station can deal with these issues, e.g., using high voltage DC breakers for LCC inverters (CIGRE B4-52 Working Group, 2011).

Meshed LCC-based DC transmission lines are difficult to operate and to control (Rodriguez & Rouzbehi, 2017; Van Hertem & Ghandhari, 2010) as, for example, LCCs and all the connected DC lines must be fully de-energized for fault recovery or to change direction of the power flow (Franck, 2011). For these reasons, we impose point-to-point configurations for LCC-based DC lines. This configuration is the most commonly used for LCC-based DC transmission lines (Bahrman & Johnson, 2007; Franck, 2011). Let $\mathcal{L}^{\text{DC}}$ denote the set of DC lines. The point-to-point constraint is then given by

$$\begin{aligned}\eta_i + \sum_{j:ij\in\mathcal{L}^{\text{DC}}} \eta_j &= \eta_i + \sum_{ij\in\mathcal{E}} \eta_j B_{ij}^0 + \sum_{ij\in\mathcal{L}\setminus\mathcal{E}} \eta_j \mu_{ij}^{\text{DC}}\\ &\leq 2,\end{aligned} \tag{40}$$

for all $i = 1, 2, \ldots, N$. Constraint (40) is bilinear. To linearize (40), we substitute the continuous variable τ_{ij} for the bilinear term. For pre-existing lines $ij \in \mathcal{E}$, we have

$$\tau_{ij} = \eta_j B^0_{ij}. \tag{41}$$

Note that B^0_{ij} is a parameter and not a variable. For all other corridor $ij \in \mathcal{L}\backslash\mathcal{E}$, we use the below disjunctive constraint:

$$\left|\tau_{ij} - \mu^{\text{DC}}_{ij} + \left(1 - \eta_j\right)\right| \leq M\left(1 - \mu^{\text{DC}}_{ij}\right) \tag{42}$$

$$\left|\tau_{ij}\right| \leq M\mu^{\text{DC}}_{ij}, \tag{43}$$

where M is a large constant. We thus re-formulate (40) as:

$$\eta_i + \sum_{j=1}^{N} \tau_{ij} \leq 2, \tag{44}$$

for all $i \in \mathcal{N}$. We remark that this constraint prohibits meshed configurations with more than two LCCs, but allows two LCCs in point-to-point configuration to have additional connections to VSCs. We could modify this constraint to prohibit LCCs in any meshed configuration, i.e., LCCs with connections to more than one other converter regardless of type. This would involve replacing η_j in (40) with ξ_j, and reformulating (41)–(44) accordingly.

We model the losses of an LCC converter similarly to the VSC cases. The real power balance equation for an LCC converter is:

$$p^{t,\text{toDC}}_i - p^{t,\text{LCC,loss,AC–DC}}_i = -p^{t,\text{toAC}}_i + p^{t,\text{LCC,loss,DC–AC}}_i.$$

No reactive power can be absorbed or injected by an LCC converter:

$$q^{t,\text{toDC}}_i = 0.$$

Thus, from (35), the apparent power constraint reduces to:

$$p^{t,\text{toDC}}_i \leq \left|\bar{J}_i\right|,$$

where $\bar{J}_i$ is the maximum current that can flow through the LCC at node i.

2.5.3. Expansion

We now formulate the power converter expansion constraints based on Sections 2.5.1 and 2.5.2. Recall that for $\xi_i = 1$, $\eta_i = 1$ if the converter is an LCC and 0 if it is a VSC, and for $\xi_i = 0$, no converter is located at node i. The type of converter must only be decided if a converter is present a node i:

$$\eta_i \leq \xi_i \tag{45}$$

Note that (45) is not essential but subsequently simplifies the model. With this constraint, a node i has VSC(s) if $\xi_i - \eta_i = 1$. Let $n^{0,\text{VSC}}_i$ be the number or size of the already installed VSCs at node i and n^{VSC}_i the number of new converters to install. We define $n^{0,\text{LCC}}_i$ and n^{LCC}_i similarly. If there are no VSCs or LCCs already present at node i, then $n^{0,\text{VSC}}_i = 0$ and $n^{0,\text{LCC}}_i = 0$. The converter expansion variables are constrained by:

$$n^{\text{VSC}}_i \leq \bar{n}^{\text{VSC}}_i(\xi_i - \eta_i) \tag{46}$$

$$n^{\text{VSC}}_i \geq \xi_i - \eta_i \tag{47}$$

$$n^{\text{LCC}}_i \leq \bar{n}^{\text{LCC}}_i \eta_i \tag{48}$$

$$n^{\text{LCC}}_i \geq \eta_i, \tag{49}$$

where $\bar{n}^{\text{VSC}}_i$ and $\bar{n}^{\text{LCC}}_i$ are the maximum number of converters at node i. Note (47) and (49) ensure that at least one converter of the appropriate type is built. Power can only be sent to or from the DC network if converters are present at node i. This translates to the following constraints:

$$\left|p^{t,\text{toDC}}_i\right| \leq M\left(n^{0,\text{VSC}}_i(\xi_i - \eta_i) + n^{\text{VSC}}_i + n^{0,\text{LCC}}_i\eta_i + n^{\text{LCC}}_i\right) \tag{50}$$

$$\left|p^{t,\text{toAC}}_i\right| \leq M\left(n^{0,\text{VSC}}_i(\xi_i - \eta_i) + n^{\text{VSC}}_i + n^{0,\text{LCC}}_i\eta_i + n^{\text{LCC}}_i\right) \tag{51}$$

$$\left|q^{t,\text{toDC}}_i\right| \leq M\left(n^{0,\text{VSC}}_i(\xi_i - \eta_i) + n^{\text{VSC}}_i\right). \tag{52}$$

The term $(\xi_i - \eta_i)$ is multiplied by $n^{0,\text{VSC}}_i$ in (50)–(52) to model scenarios in which the VSC at i is replaced by an LCC converter. If $\xi_i - \eta_i = 1$, the first term cancels and the already installed VSCs are removed from node i. Similarly, we use $n^{0,\text{LCC}}_i\eta_i$ in (50) and (51) for LCC converters replaced by VSCs. The apparent power constraints for node i for the expansion problem are:

$$\left(p^{t,\text{toDC}}_i\right)^2 + \left(q^{t,\text{toDC}}_i\right)^2 \leq \bar{I}^2_i\left(n^{0,\text{VSC}}_i(\xi_i - \eta_i) + n^{\text{VSC}}_i\right)^2 + K(1 - \xi_i + \eta_i) \tag{53}$$

$$\left(p^{t,\text{toDC}}_i\right)^2 \leq \bar{J}^2_i\left(n^{0,\text{LCC}}_i\eta_i + n^{\text{LCC}}_i\right)^2 + K(1 - \eta_i), \tag{54}$$

where K is a large positive scalar. The reactive power flow constraints are now:

$$q^{t,\text{toDC}}_i \geq -(s^0_i(\xi_i - \eta_i) + s_i)\bar{v}_i(\bar{v}_i - 1) \tag{55}$$

$$q^{t,\text{toDC}}_i \leq \alpha_i S^{\text{c,nominal}}_i\left(n^{0,\text{VSC}}_i(\xi_i - \eta_i) + n^{\text{VSC}}_i\right), \tag{56}$$

with

$$s_i \leq \bar{s}(\xi_i - \eta_i) \tag{57}$$

$$s_i \geq 0. \tag{58}$$

We only add phase reactors if a VSC is present. To ensure this, we use the expressions $(\xi_i - \eta_i)$ in (55) and (57) to activate, deactivate or allow for a new phase reactor. Lastly, four converter loss terms are needed to model LCC and VSC losses for inverters and rectifiers. We have

$$p^{t,\text{VSC,loss,AC–DC}}_i \geq 0 \tag{59}$$

$$p^{t,\text{VSC,loss,AC–DC}}_i \leq M(\xi_i - \eta_i) \tag{60}$$

$$\begin{aligned} p^{t,\text{VSC,loss,AC–DC}}_i \geq\ & a^{\text{VSC,AC–DC}}_i(\xi_i - \eta_i) \\ & + b^{\text{VSC,AC–DC}}_i\left(\left|p^{t,\text{toDC}}_i\right| + \left|q^{t,\text{toDC}}_i\right|\right) \\ & + c^{\text{VSC,AC–DC}}_i\left(\left(p^{t,\text{toDC}}_i\right)^2 + \left(q^{t,\text{toDC}}_i\right)^2\right) \\ & - M(1 - \xi_i + \eta_i) - M\left(1 - \psi^t_i\right) \end{aligned} \tag{61}$$

$$p^{t,\text{VSC,loss,DC–AC}}_i \geq 0 \tag{62}$$

$$p^{t,\text{VSC,loss,DC–AC}}_i \leq M(\xi_i - \eta_i) \tag{63}$$

$$\begin{aligned} p^{t,\text{VSC,loss,DC–AC}}_i \geq\ & a^{\text{VSC,DC–AC}}_i(\xi_i - \eta_i) \\ & + b^{\text{VSC,DC–AC}}_i\left(\left|p^{t,\text{toDC}}_i\right| + \left|q^{t,\text{toDC}}_i\right|\right) \\ & + c^{\text{VSC,DC–AC}}_i\left(\left(p^{t,\text{toDC}}_i\right)^2 + \left(q^{t,\text{toDC}}_i\right)^2\right) \\ & - M(1 - \xi_i + \eta_i) - M\psi^t_i \end{aligned} \tag{64}$$

$$p^{t,\text{LCC,loss,AC–DC}}_i \geq 0 \tag{65}$$

$$p^{t,\text{LCC,loss,AC–DC}}_i \leq M\eta_i \tag{66}$$

$$p^{t,\text{LCC,loss,AC–DC}}_i \geq a^{\text{LCC,AC–DC}}_i\eta_i + b^{\text{LCC,AC–DC}}_i\left|p^{t,\text{toDC}}_i\right|$$

$$+ c_i^{\text{LCC,AC-DC}}\left(p_i^{t,\text{toDC}}\right)^2 - M(1-\eta_i) - M\left(1-\psi_i^t\right) \tag{67}$$

$$p_i^{t,\text{LCC,loss,DC-AC}} \geq 0 \tag{68}$$

$$p_i^{t,\text{LCC,loss,DC-AC}} \leq M\eta_i \tag{69}$$

$$p_i^{t,\text{LCC,loss,DC-AC}} \geq a_i^{\text{LCC,DC-AC}}\eta_i + b_i^{\text{LCC,DC-AC}}\left|p_i^{t,\text{toDC}}\right| + c_i^{\text{LCC,DC-AC}}\left(p_i^{t,\text{toDC}}\right)^2 - M(1-\eta_i) - M\psi_i^t. \tag{70}$$

2.6. Reactive power placement

We include reactive power placement (RPP) for several reasons: (i) LCCs cannot provide and may sometimes consume reactive power, thus making it impractical to consider LCCs without RPP, and (ii) satisfying reactive power constraints locally can lead to better solutions because it can reduce the number of new lines needed (Hemmati et al., 2013; Hooshmand, Hemmati, & Parastegari, 2012; Rahmani, Rashidinejad, Carreno, & Romero, 2010). Capacitor banks can inject reactive power locally to reduce the amount that must be carried by the lines. Let $\chi_i = 1$ if a capacitor bank is installed at node i and 0 otherwise. The binary variable for RPP is necessary to model the fixed cost of building capacitor bank (see (82) in Section 3.1). The reactive power injected by the capacitor bank to node i, q_i^{cb}, is:

$$q_i^{\text{cb}} = \frac{|v_i|^2}{wC_i^{\text{total}}}, = \frac{1}{wC_i^{\text{total}}},$$

because $|v_i| = 1$ and where C_i^{total} is the total capacitance at i. Let $x_i \in \mathbb{R}$ be the reactance of the capacitor bank. The reactive power injected is then given by

$$q_i^{\text{cb}} = x_i^0 + x_i,$$

where x_i^0 is the initial reactance of the capacitor bank and $x_i \in \mathbb{R}_+$ is a continuous variable.

2.6.1. Expansion

The reactive power planning expansion constraints are:

$$x_i \leq \chi_i \bar{x} \tag{71}$$

$$x_i \geq 0 \tag{72}$$

$$q_i^{\text{cb}} = x_0 + x_i, \tag{73}$$

where $\bar{x} \in \mathbb{R}_+$ is the maximum reactance of a capacitor bank.

2.7. Generation and load

Let $g_{p,i}^t \in \mathbb{R}_+$ and $g_{q,i}^t \in \mathbb{R}$ be the real and reactive power generation variable for node i and time t. Let $g_i^{t,\text{DC}} \in \mathbb{R}_+$ be the DC power generated at node i and time t. The generation is constrained by operational limits:

$$\underline{g}_{p,i} \leq g_{p,i}^t \leq \bar{g}_{p,i} \tag{74}$$

$$\underline{g}_{q,i} \leq g_{q,i}^t \leq \bar{g}_{q,i} \tag{75}$$

$$\underline{g}_i^{\text{DC}} \leq g_i^{t,\text{DC}} \leq \bar{g}_i^{\text{DC}}, \tag{76}$$

where $\underline{g}_{p,i}$ and $\bar{g}_{p,i}$ are the minimum and maximum active power generation at i, $\underline{g}_{q,i}$ and $\bar{g}_{q,i}$ are the minimum and maximum reactive power generation at i and $\underline{g}_i^{\text{DC}}$ and $\bar{g}_i^{\text{DC}}$ are the minimum and maximum DC power generation at i. If no generators are present at node i, then the upper bounds of (74)–(76) are set to zero. Let $d_{p,i}^t$ and $d_{q,i}^t$ be the active and reactive power demand at node i and time t. Let $d_i^{t,\text{DC}}$ be the DC power demand at node i and time t. Each node $i \in \mathcal{N}$ must satisfy the following balance equations:

$$p_i^t = g_{p,i}^t - d_{p,i}^t - p_i^{t,\text{toDC}} \tag{77}$$

$$q_i^t = g_{q,i}^t - d_{q,i}^t - q_i^{t,\text{toDC}} + q_i^{\text{cb}} \tag{78}$$

$$p_i^{t,\text{DC}} = g_{\text{DC},i}^t - d_i^{t,\text{DC}} - p_i^{t,\text{toAC}} \tag{79}$$

$$p_i^{t,\text{toDC}} - p_i^{t,\text{VSC,loss,AC-DC}} - p_i^{t,\text{LCC,loss,AC-DC}} = -p_i^{t,\text{toAC}} + p_i^{t,\text{VSC,loss,DC-AC}} + p_i^{t,\text{LCC,loss,DC-AC}}. \tag{80}$$

2.8. Active power loss

The active power loss of the entire network is sometimes a useful performance measure in planning. Let ℓ^t denote the total active power loss time t. The losses are given by the sum of the resistive losses and converter losses:

$$\ell^t = \sum_{ij\in\mathcal{L}}\left(P_{ij}^t + P_{ji}^t + P_{ij}^{t,\text{DC}} + P_{ji}^{t,\text{DC}}\right) + \sum_{i\in\mathcal{N}}\left(p_i^{t,\text{VSC,loss,AC-DC}} + p_i^{t,\text{LCC,loss,AC-DC}} + p_i^{t,\text{VSC,loss,DC-AC}} + p_i^{t,\text{VSC,loss,DC-AC}}\right). \tag{81}$$

Total active power losses are then $\sum_{t=1}^T \ell^t$.

3. Costs

3.1. Expansion costs

Let c_{ij}^{AC} and c_{ij}^{DC} be the costs of AC and DC lines in corridor ij. Let $c_{ij}^{\text{AC-DC}}$, $ij \in \mathcal{E}$, be the cost of converting an AC line to DC. Let d_i^{VSC}, and d_i^{LCC} be the costs of converters at node i. The converter costs can depend on the node variable installation costs, e.g., for offshore wind turbines, or the required specialized hardware, e.g., for solar photovoltaics. We assume that the cost of an AC–DC converter is the same as a DC–AC converter. Let c_i^{cb} and c_i^{b} be the marginal cost associated with capacitor banks and susceptance size of the VSC station at node i, respectively, and $c_i^{\text{cb},0}$ be the fixed cost associated with a new capacitor bank at node i. Note that line costs depend on the distance and geographical features between buses. Converter costs are allowed to vary with the bus to reflect details such as the specialized converters used in solar farms, and the added expense of installing converters on offshore wind platforms. The total expansion cost is a function of $\mathcal{V} = \{v_{ij}^{\text{AC}}, v_{ij}^{\text{DC}}, \phi_{ij}^{\text{AC-DC}}, n_i^{\text{VSC}}, n_i^{\text{LCC}}, \chi_i, x_i, s_i|$ for all $i, j \in \mathcal{N}, ij \in \mathcal{L}$ and $t = 1, 2, \ldots, T\}$. The total expansion cost function $e : \mathcal{V} \mapsto \mathbb{R}_+$ is

$$e(\mathcal{V}) = \sum_{ij\in\mathcal{L}}\left(c_{ij}^{\text{AC}}v_{ij}^{\text{AC}} + c_{ij}^{\text{DC}}\left(v_{ij}^{\text{DC}} - \phi_{ij}^{\text{AC-DC}}\right)\right) + \sum_{ij\in\mathcal{E}}\left(c_{ij}^{\text{AC-DC}}\phi_{ij}^{\text{AC-DC}}\right) + \sum_{i\in\mathcal{N}}\left(d_i^{\text{VSC}}n_i^{\text{VSC}} + d_i^{\text{LCC}}n_i^{\text{LCC}} + c_i^{\text{cb},0}\chi_i + c_i^{\text{cb}}x_i + c_i^{\text{b}}s_i\right). \tag{82}$$

Table 4
AC-DC expansion planning computation time for the different bus systems.

Bus System	Computation time [min]
AC–DC Garver with RPP	2.61
AC–DC Garver with long transmission lines	3.81
AC–DC Garver with DC generation	9.36
AC–DC IEEE 24-bus reliability system with DC nodes	228.61

3.2. Generation costs

Let $\mathcal{G}^{\text{AC}} \subseteq \mathcal{N}$ be the set of AC generators. If $i \notin \mathcal{G}^{\text{AC}}$, then $g^t_{p,i} = g^t_{q,i} = 0$ for all t. The generation cost $f : \mathbb{R}_+ \mapsto \mathbb{R}_+$ is assumed to be given by the fuel function:

$$f_i(g^t_{p,i}) = a^{\text{g}}_i + b^{\text{g}}_i g^t_{p,i} + c^{\text{g}}_i \left(g^t_{p,i}\right)^2,$$

where a^{g}_i, b^{g}_i and c^{g}_i are positive scalar. The total generation cost is $\sum_{t=1}^{T} \sum_{i \in \mathcal{G}^{\text{AC}}} f_i(g^t_{p,i})$.

4. Expansion problem formulation

Let

$$\begin{aligned}\mathcal{X} = \Big\{ & p^t_i, q^t_i, p^{t,\text{DC}}_i, p^{t,\text{toDC}}_i, q^{t,\text{toDC}}_i, p^{t,\text{toAC}}_i, p^{t,\text{VSC,loss,AC–DC}}_i, \\ & p^{t,\text{VSC,loss,DC–AC}}_i, p^{t,\text{LCC,loss,AC–DC}}_i, p^{t,\text{LCC,loss,DC–AC}}_i, q^{\text{cb}}_i, P^t_{ij}, Q^t_{ij}, \\ & P^{t,\text{DC}}_{ij}, \mu^{\text{AC}}_{ij}, \mu^{\text{DC}}_{ij}, \tau_{ij}, \lambda_i, \kappa_i, \xi_i, \eta_i, \psi^t_i, g^t_{p,i}, g^t_{q,i}, g^{t,\text{DC}}_i, b_i, \ell^t_i \Big| \\ & \text{for all } i, j \in \mathcal{N}, ij \in \mathcal{L} \text{ and } t = 1, 2, \ldots, T \Big\} \cup \mathcal{V}\end{aligned}$$

be the set of optimization variables. Let β and δ be positive scalars. The expansion problem is a mixed-integer second order cone program (MISOCP) given by

$$\begin{aligned} \min_{\mathcal{X}} \quad & e(\mathcal{V}) + \beta \sum_{t=1}^{T} \ell^t + \delta \sum_{t=1}^{T} \sum_{i \in \mathcal{G}^{\text{AC}}} f_i(g^t_{p,i}) \\ \text{subject to} \quad & (1), (4) - (22), \\ & (27) - (34), \\ & (37) - (38), \\ & (41) - (81), \\ & \text{for all } i \in \mathcal{N}, ij \in \mathcal{L} \text{ and } t = 1, 2, \ldots, T. \end{aligned} \tag{83}$$

5. Case study

We test the model (83) on two different networks: the AC–DC 6-bus Garver system (Garver, 1970; Rider, Garcia, & Romero, 2007) and the AC–DC IEEE 24-bus reliability test system (Grigg et al., 1999; Rider et al., 2007). We use `CVXPY` (Akshay Agrawal & Boyd, 2018; Diamond & Boyd, 2016) and the commercial solver `Gurobi` (Gurobi Optimization, 2018) on a 2.7 GHz Intel Core i5 laptop for all computations. The computation times for all simulations are shown in Table 4.

The 6-bus Garver system was first presented in Garver (1970). The AC–DC Garver system data are gathered in Table SM.1 of the Supplementary Materials. The AC line parameters are detailed in Rider et al. (2007), and we have created parameters for the DC lines and converters as follows. The resistance and cost of a DC line are computed using the ratio of AC to DC resistance and cost, respectively, from Wu et al. (2018) and Lotfjou et al. (2012). We use the total cost per line corridor instead of per kilometer cost because it can account for factors like corridor specific maintenance and natural obstacles. The per unit line capacity of the AC and DC lines is set to be the same. The AC to DC line conversion costs are set to half the DC line costs, as it is estimated in Häusler, Schlayer, and Fitterer (1997).

Table 5
Optimal value of the different terms of the expansion problem for the AC–DC Garver system.

Garver system	Expansion [M$]	Losses [M$]	Generation [M$]
With RPP	110.24	0.26	701.52
With long transmission lines	749.47	1.72	768.06
With DC generation	401.79	0.88	108.50

Table 6
Optimal expansion plan for the AC–DC Garver system.

Branch	ν^{AC}_{ij}	ν^{DC}_{ij}	$\nu^{\text{strictlyAC}}_{ij}$
2–3	1	0	1
2–6	1	0	1
3–5	1	0	1
4–6	2	0	2

The 24-bus system was originally given in Grigg et al. (1999) and adapted for transmission expansion in Rider et al. (2007). Its parameters are given in Table SM.2 of the Supplementary materials. The DC values are obtained the same way as for the 6-bus system. The generation and demand parameters are set to be twice as large as the original values from Grigg et al. (1999) (or 2/3 the values in Rider et al. (2007)). Thus, expansion is required for the system to admit a feasible power flow. The generation costs are taken from Zimmerman, Murillo-Sánchez, Thomas et al. (2011), aggregated and simplified so that each generator node has a single set of cost parameters.

The costs and parameters of VSCs and LCCs are the same for all nodes and for both systems, and are given in Table SM.3 of the Supplementary Materials. The VSC parameters are from Beerten et al. (2010). We approximate the LCC loss coefficient as half the value of the VSC to represent their lower losses (Van Eeckhout, 2008). The current limit of an LCC converter is taken to be equal to the VSC value. The cost per kVA of VSC is given in Wu et al. (2018). The LCC costs are scaled down according to the comparison in Lazaridis (2005). The parameter α for each converter is is set to 0.5 and $S^{\text{c,nominal}}_i$ to 1 p.u. (Bahrami et al., 2017). We assume that the capacitor bank and phase reactor costs are the same and let $c^{\text{cb}}_i = c^{\text{b}}_i = 0.003M/MVAR and $c^{\text{cb,0}}_i = 0.001$ M$ (Hooshmand et al., 2012; Rahmani et al., 2010) for all nodes i.

We compare the optimal AC–DC expansion plan to a strictly AC expansion plan. The strictly AC expansion model is equivalent to the branch flow-based second-order cone (BFSOC) model from Taylor and Hover (2013) when no converters are needed. The superscript 'striclyAC' denotes an expansion plan from this model.

5.1. AC–DC Garver system

We solve the model (83) on the AC–DC Garver system described in Table SM.1 of the Supplementary Materials. We set $\beta = 1$ and $\delta = 0.1$ in the objective function of (83). In all simulations with the Garver system, we consider three demand scenarios: off-peak ($t = 0$), mid-peak ($t = 1$) and peak ($t = 2$) demand with active and reactive power demand equal to respectively half the values in Table SM.1 of the Supplementary materials, three quarters of their values and their full values. The expansion plans for all Garver system examples are summarized in Fig. 1. The optimal values of the three terms of (83)'s objective function are presented in Table 5.

For the Garver system, we first consider the case with no reactive power placement. The optimal expansion plan is summarized in Table 6. As shown in Table 6, the expansion plan for our AC–DC expansion model without reactive power planning and the BFSOC are the same: transmission lines are built in the same corridor and in the same quantity. The expansion cost (82) in both

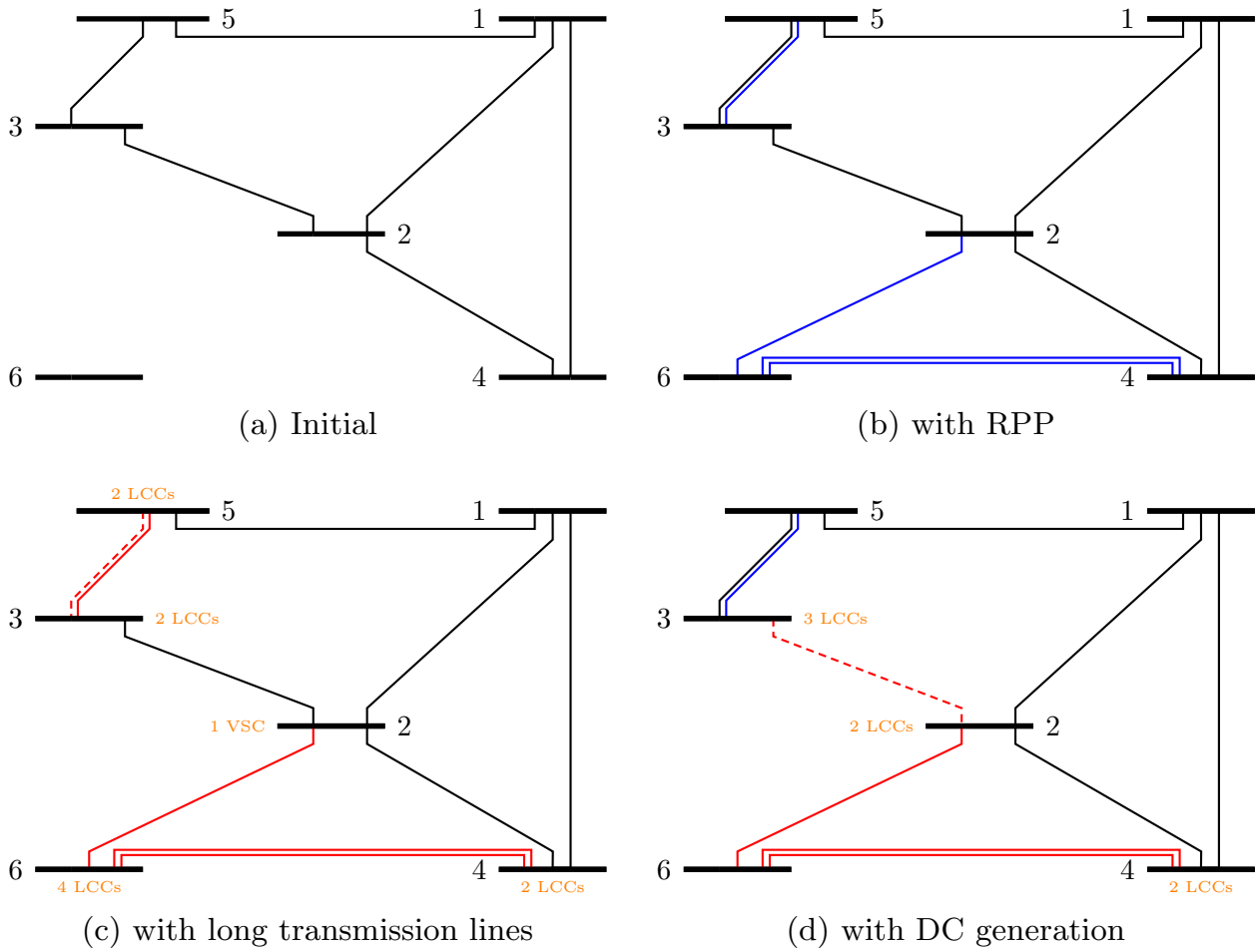

Fig. 1. Expansion plan for different AC–DC Garver systems (*black: original line, blue: AC line, red: DC line, orange: converter, dashed: line conversion.*) (For interpretation of the references to colour in this figure, the reader is referred to the web version of this article.)

cases is 130.00. In this case, no DC lines nor converters are built as there is no financial advantage to DC expansion. This is due to the short distances between buses and the absence of DC generation. We give examples with greater distances between buses and DC generation in the next subsections.

When reactive power planning is considered, the expansion cost decreases to 110.24. The optimal expansion plan with RPP is presented in Figure 1b. At this time, no line is built in the 2–3 corridor as the need to transport reactive power is reduced. The optimal value of the expansion cost, loss and generation terms of the expansion objective function are presented in Table 5, first line. Note that for all the following expansions, RPP is always considered.

5.1.1. System with long transmission lines

We now consider a version of the Garver network with lines that are six times as long. All line resistances, reactances, and costs are set to six times the value given in Table SM.2 of the Supplementary materials. We chose this larger size range to reflect the so-called break-even distance at which DC lines become cheaper than AC. The expansion plans for both the AC–DC and strictly AC models are presented in Table 7 and illustrated in Fig. 1(c). The optimal objective is also detailed in Table 5. The expansion costs for the AC–DC and strictly AC expansion plans are 749.47 and 1441.80, respectively. The AC–DC expansion leads to a 48% cost reduction and consists only of DC lines. Additionally, the AC line in the corridor 3–5 is converted to DC. Also note that only five lines are needed for AC–DC expansion, whereas purely AC expansion requires nine. This is due to the large reactive power losses of long AC transmission lines. Finally, we observe that although the direction of the power flow is the same in all scenarios, the point-to-point requirement of LCC-interfaced lines requires that a VSC be present at node 2.

Table 7
Optimal expansion plan for the AC–DC Garver system with long transmission lines.

Branch	v_{ij}^{AC}	v_{ij}^{DC}	ϕ_{ij}^{ACDC}	$v_{ij}^{AC,strictlyAC}$
2 – 3	0	0	0	1
2 – 6	0	1	0	3
3 – 5	0	2	1	2
4 – 6	0	2	0	3
Node	n_i^{LCC}	n_i^{VSC}	$n_i^{LCC,strictlyAC}$	$n_i^{VSC,strictlyAC}$
1	0	0	0	0
2	0	1	0	0
3	2	0	0	0
4	2	0	0	0
5	2	0	0	0
6	4	0	0	0

5.1.2. Network with DC generation

Lastly, we consider an example with DC power generation and medium length transmission lines. In this case, the AC and DC resistances, reactances and costs are multiplied by three. The generators at nodes 3 and 6 are replaced by DC generators, e.g., large PV arrays, with capacities of respectively, 400 and 250 MW. The expansion plan is shown in Fig. 1(d) and in Table 8. The expansion

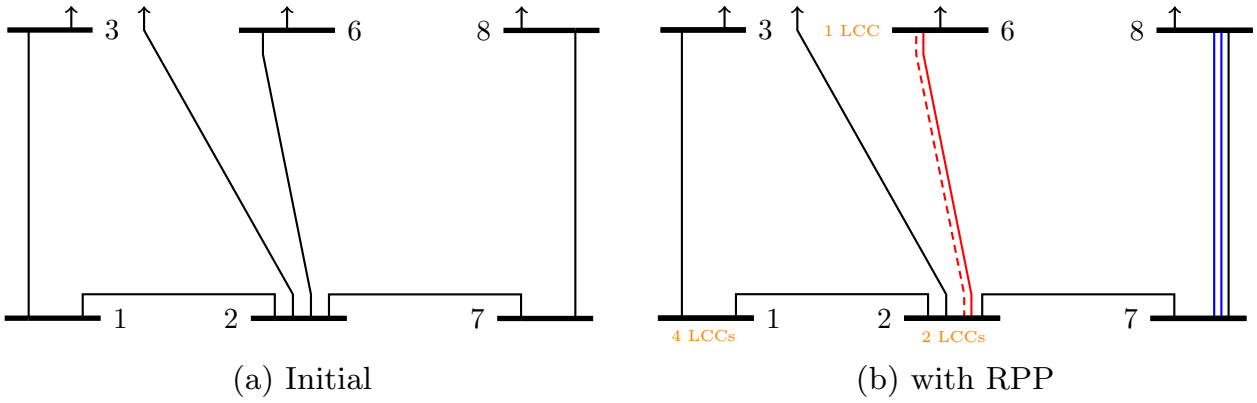

Fig. 2. Expansion plan for the AC–DC IEEE 24-bus reliability system with DC nodes (*black: original line, blue: AC line, red: DC line, orange: converter, dashed: line conversion, arrow: connection with remainder of the network.*) (For interpretation of the references to colour in this figure, the reader is referred to the web version of this article.)

Table 8
Optimal expansion plan for the AC–DC Garver system with DC generation.

Branch	ν_{ij}^{AC}	ν_{ij}^{DC}	ϕ_{ij}^{ACDC}	$\nu_{ij}^{AC,striclyAC}$
2–3	0	1	1	1
2–6	0	1	0	1
3–5	1	0	0	2
4–6	0	2	0	2
Node	n_i^{LCC}	n_i^{VSC}	$n_i^{LCC,strictlyAC}$	$n_i^{VSC,strictlyAC}$
1	0	0	0	0
2	2	0	0	0
3	3	0	4	0
4	2	0	0	0
5	0	0	0	0
6	0	0	3	0

Table 9
Optimal expansion plan for the 24-bus reliability system with DC nodes.

Branch	ν_{ij}^{AC}	ν_{ij}^{DC}	ϕ_{ij}^{ACDC}	$\nu_{ij}^{AC,striclyAC}$
1–2	0	0	0	1
2–6	0	2	1	2
7–8	2	0	0	3
Node		n_i^{LCC}	n_i^{VSC}	$n_i^{LCC,strictlyAC}$
1		4	0	4
2		2	0	4
5		0	0	0
6		1	0	3
7		0	0	0
8		0	0	0

Table 10
Optimal value of the different terms of the expansion problem for the AC–DC IEEE 24-bus reliability system.

IEEE 24-bus reliability system	Expansion [M$]	Losses [M$]	Generation [M$]
With DC nodes	282.58	6.51	224.88

planning (83) objective term values are given in Table 5. The AC–DC plan is compared to a strictly AC plan in which converters may be built at nodes to accommodate DC generation, but no DC lines are permitted.

The cost of the AC–DC and strictly AC plans in this case are 401.79 and 541.99, respectively, and represents a reduction of 26%. A combination of AC and DC lines are installed. No converter is installed at node 6, and its DC generation is carried by newly installed DC lines. On the other hand, LCCs are installed at node 3, where there is another DC generator, and the power is carried by a combination of AC and DC lines.

5.2. AC–DC IEEE 24-bus reliability system with DC nodes

We now apply the expansion model to a modified version of the IEEE 24-bus reliability system. The generators at node 1 and 2 are replaced by DC generators, node 6 is converted to a DC load, and we make the transmission lines twice as long as in Table SM.2 of the Supplementary materials and Grigg et al. (1999). This network consists of 24 nodes and 41 line corridors. Assigning an expansion corridor between every node pair would lead to a prohibitively large problem. We instead limit the installation of new lines and line conversions to those connected to a subset of nodes, $\mathcal{C} = \{1, 2, 3, 6, 7, 8\}$. All nodes can be equipped with capacitor banks, and we let the maximum reactive power of a capacitor bank be $\bar{x} = 1000$ MVAr, which can satisfy all reactive power needs locally. We set $\beta = 1$ and $\delta = 10^{-2}$ so the generation and expansion cost terms of (83) have the same order of magnitude.

We consider two demand scenarios: off-peak ($t = 0$) and on peak ($t = 1$) with demand values respectively equivalent to half and the full values given in Table SM.2 of the Supplementary Materials. We solve with the candidate line corridors implied by $\mathcal{C}$.

We present the optimal expansion plan in Fig. 2 and Table 9 and compare it to a strictly AC expansion plan. We show the optimal expansion, loss, and generation terms in Table 10. The total expansion cost for the AC–DC expansion is 282.58 and 448.21 for the strictly AC expansion. This represents a 37% reduction in costs. In this case, the AC–DC expansion can reduce the total number of lines required from 6 for a strictly AC expansion to 4 by converting the line in corridor 2–6 to a DC line. Four LCCs are built at node 1, a DC power generator. These converters have the same costs as standard LCCs, but could be modified to reflect the converters used in DC generators like wind or solar farms. For conciseness, we omit this aspect in our case study, but we note that our model is compatible with this level of detail.

6. Expansion feasibility

We now discuss the feasibility of expansion plans produced by our model. Because (83) is based on an SOC relaxation and fixing nodal voltages to one per unit, it can produce solutions that are infeasible with respect to the original nonconvex expansion planning problem. This can be due to, for example, underestimated power losses, thus leading to fewer lines than needed in a given corridor. An infeasible plan can be used as a starting point for a mixed-integer nonlinear programming solver, thus reducing the chances of finding a bad local minimum. It is common for solutions from mixed-integer convex transmission expansion models

Table 11
Feasibility results.

Example	Reinforcement	rank $\mathbf{V}^t$	$\lambda_1(\mathbf{V}^t)/\lambda_2(\mathbf{V}^t), t = 1, 2, 3$
Garver with RPP	–	$= 1$	–
Garver with long transmission lines	$\nu_{26}^{DC} + 1$ $n_2^{VSC} + 1$ $n_3^{LCC} + 1$	> 1	7.2%, 1.9×10^{-2}%, 2.5%
Garver with DC generation	$\nu_{23}^{DC} + 1$ $n_2^{LCC} + 1$	≥ 1	3.7%, 5.0×10^{-5}%, 1.5×10^{-5}%
24-bus system with DC nodes	–	> 1	1.2%, 7.4×10^{-4}%

to require reinforcement to attain feasibility (Taylor & Hover, 2011, 2013). Transmission expansion is not a real-time decision process. There is ample time to refine solutions produced by the MISOC model, as well as to compare with solutions produced by other approaches. For example, a nonlinear solver with our solution as its initial point could be used to obtain feasible and improved plans prior to actual deployment.

We use the semidefinite relaxation (SDR) of Bahrami et al. (2017) to assess the feasibility of the transmission plans produced by (83). More precisely, if the relaxation variable in the solution to the SDR for the expansion plan has rank one, then the expansion plan admits a feasible power flow, and is therefore feasible itself. If the rank is not one, we look at the ratio of the largest and second-largest eigenvalues to estimate how close to feasible the solution is. We remark that it would be ideal to assess feasibility via a nonlinear load flow. Unfortunately, there is limited literature on load flow with AC and DC lines, and, moreover, no standard software packages. Given that load flow itself is not our focus, we have therefore used the SDR of Bahrami et al. (2017), the setup of which is relatively close to our own. To use the SDR relaxation of Bahrami et al. (2017), we made the following two modifications: (i) LCCs are included as well as VSCs, and (ii) multiple AC lines can connect to power converter nodes because the filter node is modeled as a part of the converter. These two aspects are modeled using the same converter loss constraints (59)–(70) as in the expansion model and by removing the current relaxation variable of Bahrami et al. (2017). In all feasibility computations, capacitor bank reactances can be re-optimized. The full formulation is given in (SM.1) of the Supplementary materials.

We use the parser `CVXPY` (Akshay Agrawal & Boyd, 2018; Diamond & Boyd, 2016) and the solver `MOSEK` (MOSEK ApS, 2017) for all feasibility computations. We solve the SDR on the optimal expansion plan computed in Section 5 for the three versions of the Garver system and the modified 24-bus reliability system. If an optimal expansion plan is infeasible with respect to the SDR, minor reinforcement is used on the expansion. In all cases, we compute the rank of the semidefinite variable for all t. If the rank is greater than one, then we compute the ratio of the largest to the second largest eigenvalue of the semidefinite variables for all t. The feasibility results are presented in Table 11.

In the case of the Garver system with RPP, the optimal voltage matrix $\mathbf{V}^t$ has rank one (with a tolerance of 10^{-5}) for all t. In this case, the relaxation is exact and the expansion plan is feasible. In all the other examples, the rank is not one, but the ratios of eigenvalues for the the semidefinite variable indicates that the solution is close to feasible. In both the Garver system with long lines and with DC generation, the addition of a single DC line and corresponding converters was needed to make the relaxation feasible.

7. Conclusion

We have formulated a mixed-integer second-order cone transmission expansion planning model for AC–DC networks. We model AC and DC power flow using the branch flow model with unit voltage magnitudes at all nodes. Our model includes line conversion, reactive power placement, and VSCs and LCCs. The result is an MISOCP, which can be solved to optimality using commercial solvers. We present numerical results on 6-bus and 24-bus networks. For a 6-bus network with long transmission lines, the AC–DC expansion cost is almost 50% lower than when only AC lines are allowed. Our MISOC expansion planning model is based on relaxations and approximations. For these reasons, it may produce infeasible solutions with respect to the original nonconvex planning problem. We use a semidefinite relaxation of power flow to assess the feasibility of the expansion plans produced by our model, and find the the plans produced by our model are either feasible or nearly feasible.

One could alternatively formulate an AC–DC expansion planning model based purely on relaxations, e.g., semidefinite or second-order cone relaxations (Taylor and Hover, 2013, Section II-C). This would result in a significant increase in the number of continuous variables, but could ultimately yield more accurate results. This is a topic of future work.

Acknowledgement

The Authors thank Prof. Reza Iravani for helpful discussions.

Supplementary material

Supplementary material associated with this article can be found, in the online version, at doi:10.1016/j.ejor.2019.08.016.

References

Ahmed, H. M., Eltantawy, A. B., & Salama, M. (2018a). A generalized approach to the load flow analysis of AC–DC hybrid distribution systems. *IEEE Transactions on Power Systems, 33*(2), 2117–2127.
Ahmed, H. M., Eltantawy, A. B., & Salama, M. M. (2018b). A planning approach for the network configuration of AC–DC hybrid distribution systems. *IEEE Transactions on Smart Grid, 9*(3), 2203–2213.
Agrawal, A., Diamond, S., Verschueren, R., & Boyd, S. (2018). A rewriting system for convex optimization problems. *Journal of Control and Decision, 5*(1), 42–60.
Bahrami, S., Therrien, F., Wong, V. W., & Jatskevich, J. (2017). Semidefinite relaxation of optimal power flow for AC–DC grids. *IEEE Transactions on Power Systems, 32*(1), 289–304.
Bahrman, M. P., & Johnson, B. K. (2007). The ABCs of HVDC transmission technologies. *IEEE Power and Energy Magazine, 5*(2), 32–44.
Baradar, M., Hesamzadeh, M. R., & Ghandhari, M. (2013). Second-order cone programming for optimal power flow in VSC-type AC–DC grids. *IEEE Transactions on Power Systems, 28*(4), 4282–4291.
Barnes, M., Van Hertem, D., Teeuwsen, S. P., & Callavik, M. (2017). HVDC systems in smart grids. *Proceedings of the IEEE, 105*(11), 2082–2098.
Beerten, J., Cole, S., & Belmans, R. (2010). A sequential AC/DC power flow algorithm for networks containing multi-terminal VSC HVDC systems. In *Proceedings of IEEE PES general meeting*.
Beerten, J., Cole, S., & Belmans, R. (2012). Generalized steady-state VSC MTDC model for sequential AC/DC power flow algorithms. *IEEE Transactions on Power Systems, 27*(2), 821–829.
Cao, J., Du, W., Wang, H. F., & Bu, S. (2013). Minimization of transmission loss in meshed AC/DC grids with VSC-MTDC networks. *IEEE Transactions on Power Systems, 28*(3), 3047–3055.
CIGRE B4-52 Working Group (2011). HVDC grid feasibility study. *Melbourne: International Council on Large Electric Systems*.
Daelemans, G. (2008). *VSC HVDC in meshed networks*. (Ph.D. thesis) Katholieke Universiteit Leuven.

Daelemans, G., Srivastava, K., Reza, M., Cole, S., & Belmans, R. (2009). Minimization of steady-state losses in meshed networks using VSC HVDC. In *Proceedings of IEEE PES general meeting* (pp. 971–975).

Diamond, S., & Boyd, S. (2016). CVXPY: a python-embedded modeling language for convex optimization. *Journal of Machine Learning Research, 17*(83), 1–5.

Doagou-Mojarrad, H., Rastegar, H., & Gharehpetian, G. B. (2016). Probabilistic multi-objective HVDC/AC transmission expansion planning considering distant wind/solar farms. *IET Science, Measurement & Technology, 10*(2), 140–149.

Dominguez, A. H., Macedo, L. H., Escobar, A. H., & Romero, R. (2017). Multistage security-constrained HVAC/HVDC transmission expansion planning with a reduced search space. *IEEE Transactions on Power Systems, 32*(6), 4805–4817.

Dominguez, A. H., Zuluaga, A. H. E., Macedo, L. H., & Romero, R. (2016). Transmission network expansion planning considering HVAC/HVDC lines and technical losses. In *Proceedings of IEEE PES transmission & distribution conference and exposition-latin america* (pp. 1–6).

Ergun, H., Dave, J., Van Hertem, D., & Geth, F. (2019). Optimal power flow for ac/dc grids: formulation, convex relaxation, linear approximation and implementation. *IEEE Transactions on Power Systems*.

Feng, W., Le Tuan, A., Tjernberg, L. B., Mannikoff, A., & Bergman, A. (2014). A new approach for benefit evaluation of multiterminal VSC–HVDC using a proposed mixed AC/DC optimal power flow. *IEEE Transactions on Power Delivery, 29*(1), 432–443.

Franck, C. M. (2011). HVDC circuit breakers: A review identifying future research needs. *IEEE Transactions on Power Delivery, 26*(2), 998–1007.

Frank, S. M., & Rebennack, S. (2015). Optimal design of mixed AC–DC distribution systems for commercial buildings: A nonconvex generalized Benders decomposition approach. *European Journal of Operational Research, 242*(3), 710–729.

Garver, L. L. (1970). Transmission network estimation using linear programming. *IEEE Transactions on Power Apparatus and Systems, PAS-89*(7), 1688–1697.

Ghaddar, B., & Jabr, R. A. (2019). Power transmission network expansion planning: A semidefinite programming branch-and-bound approach. *European Journal of Operational Research, 274*(3), 837–844. doi:10.1016/j.ejor.2018.10.035.

Ghadiri, A., Haghifam, M. R., & Larimi, S. M. M. (2017). Comprehensive approach for hybrid AC/DC distribution network planning using genetic algorithm. *IET Generation, Transmission & Distribution, 11*(16), 3892–3902.

Grigg, C., Wong, P., Albrecht, P., Allan, R., Bhavaraju, M., Billinton, R., Kuruganty, S., et al. (1999). The IEEE reliability test system-1996. A report prepared by the reliability test system task force of the application of probability methods subcommittee. *IEEE Transactions on Power Systems, 14*(3), 1010–1020.

Gurobi Optimization, L. (2018). Gurobi optimizer reference manual. http://www.gurobi.com.

Häusler, M., Schlayer, G., & Fitterer, G. (1997). Converting AC power lines to DC for higher transmission ratings. *ABB Review*, 4–11.

Hemmati, R., Hooshmand, R.-A., & Khodabakhshian, A. (2013). State-of-the-art of transmission expansion planning: Comprehensive review. *Renewable and Sustainable Energy Reviews, 23*, 312–319.

Henderson, M., Gagnon, J., Bertagnolli, D., Hosie, B., DeShazo, G., & Silverstein, B. (2007). Building a plan for HVDC. *IEEE Power and Energy Magazine, 5*(2), 52–60.

Hooshmand, R.-A., Hemmati, R., & Parastegari, M. (2012). Combination of AC transmission expansion planning and reactive power planning in the restructured power system. *Energy Conversion and Management, 55*, 26–35.

Lazaridis, L. (2005). *Economic comparison of HVAC and HVDC solutions for large offshore wind farms under special consideration of reliability*. (Ph.D. thesis) KTH Royal Institute of Technology.

Lotfjou, A., Fu, Y., & Shahidehpour, M. (2012). Hybrid AC/DC transmission expansion planning. *IEEE Transactions on Power Delivery, 27*(3), 1620–1628.

Lumbreras, S., & Ramos, A. (2016). The new challenges to transmission expansion planning. survey of recent practice and literature review. *Electric Power Systems Research, 134*, 19–29.

McCormick, G. P. (1976). Computability of global solutions to factorable nonconvex programs: Part Iconvex underestimating problems. *Mathematical Programming, 10*(1), 147–175.

MOSEK ApS (2017). The Mosek optimization toolbox for Matlab manual. version 8.1. http://docs.mosek.com/8.1/toolbox/index.html.

Novoa, J. P., & Rios, M. A. (2017). Conversion of HVAC lines into HVDC in transmission expansion planning. *World Academy of Science, Engineering and Technology, International Journal of Electrical, Computer, Energetic, Electronic and Communication Engineering, 11*(12), 1088–1094.

Rahmani, M., Rashidinejad, M., Carreno, E., & Romero, R. (2010). Efficient method for AC transmission network expansion planning. *Electric Power Systems Research, 80*(9), 1056–1064.

Rider, M., Garcia, A., & Romero, R. (2007). Power system transmission network expansion planning using AC model. *IET Generation, Transmission & Distribution, 1*(5), 731–742.

Rodriguez, P., & Rouzbehi, K. (2017). Multi-terminal DC grids: challenges and prospects. *Journal of Modern Power Systems and Clean Energy, 5*(4), 515–523.

Schilling, S., Kuschke, M., & Strunz, K. (2017). AC–DC optimal power flow implementation: Modeling and application to an HVDC overlay grid. In *Proceedings of IEEE Manchester powertech* (pp. 1–6).

Taylor, J. A. (2015). *Convex optimization of power systems*. Cambridge University Press.

Taylor, J. A., & Hover, F. S. (2011). Linear relaxations for transmission system planning. *IEEE Transactions on Power Systems, 26*(4), 2533–2538.

Taylor, J. A., & Hover, F. S. (2013). Conic AC transmission system planning. *IEEE Transactions on Power Systems, 28*(2), 952–959.

Urquidez, O. A., & Xie, L. (2015). Smart targeted planning of VSC-based embedded HVDC via line shadow price weighting. *IEEE Transactions on Smart Grid, 6*(1), 431–440.

Van Eeckhout, B. (2008). *The economic value of VSC HVDC compared to HVAC for offshore wind farms*. (Ph.D. thesis) Katholieke Universiteit Leuven.

Van Hertem, D., & Ghandhari, M. (2010). Multi-terminal VSC HVDC for the European supergrid: obstacles. *Renewable and Sustainable Energy Reviews, 14*(9), 3156–3163.

Wu, Z., Liu, P., Gu, W., Huang, H., & Han, J. (2018). A bi-level planning approach for hybrid AC–DC distribution system considering N-1 security criterion. *Applied Energy, 230*, 417–428.

Yang, Z., Zhong, H., Bose, A., Xia, Q., & Kang, C. (2018). Optimal power flow in AC–DC grids with discrete control devices. *IEEE Transactions on Power Systems, 33*(2), 1461–1472.

Zimmerman, R. D., Murillo-Sánchez, C. E., Thomas, R. J., et al. (2011). Matpower: steady-state operations, planning, and analysis tools for power systems research and education. *IEEE Transactions on Power Systems, 26*(1), 12–19.